HYDROLOGICAL PROCESSES
*Hydrol. Process.* **21**, 1664–1677 (2007)
Published online 23 January 2007 in Wiley InterScience
(www.interscience.wiley.com) DOI: 10.1002/hyp.6360

# Evaporation estimation on Lake Titicaca: a synthesis review and modelling

François Delclaux,[1]* Anne Coudrain[2] and Thomas Condom[3]

[1] *IRD, UMR HydroSciences Montpellier, (CNRS/IRD/UMI/UMII), MSE, F-34000 Montpellier, France*
[2] *IRD, Great Ice, MSE, F-34000 Montpellier, France*
[3] *Institut EGID, Université Bordeaux III, F-33600 Pessac, France*

## Abstract:

The aim of this study was to validate evaporation models that can be used for palaeo-reconstructions of large lake water levels. Lake Titicaca, located in a high-altitude semi-arid tropical area in the northern Andean Altiplano, was the object of this case study. As annual evaporation is about 90% of lake output, the lake water balance depends heavily on the yearly and monthly evaporation flux. At the interannual scale, evaporation estimation presents great variability, ranging from 1350 to 1900 mm year$^{-1}$. It has been found that evaporation is closely related to lake rainfall by a decreasing relationship integrating the implicit effect of nebulosity and humidity. At the seasonal scale, two monthly evaporation data sets were used: pan observations and estimations derived from the lake energy budget. Comparison between these data sets shows that (i) there is one maximum per year for pan evaporation and two maxima per year for lake evaporation, and (ii) pan evaporation is greater than lake evaporation by about 100 mm year$^{-1}$. These differences, mainly due to a water depth scale factor, have been simulated with a simple thermal model $\theta_w(h, t)$ of a free-surface water column. This shows that pan evaporation ($h = 0{\cdot}20$ m) is strongly correlated with direct solar radiation, whereas the additional maximum of lake evaporation ($h = 40$ m) is related to the heat restitution towards the atmosphere from the water body at the end of summer. Finally, five monthly evaporation models were tested in order to obtain the optimal efficiency/complexity ratio. When the forcing variables are limited to those that are most readily available in the past, i.e. air temperature and solar radiation, the best results are obtained with the radiative Abtew model ($r = 0{\cdot}70$) and with the Makkink radiative/air temperature model ($r = 0{\cdot}67$). Copyright © 2007 John Wiley & Sons, Ltd.

KEY WORDS Lake Titicaca; evaporation; pan; model; annual scale; monthly scale; radiative budget; energy budget

*Received 8 September 2005; Accepted 10 May 2006*

## INTRODUCTION

Wetland dynamics provide a suitable framework for analysing the consequences of hydrological and climatic changes, as well as the impact of human activities. More particularly, endorheic lakes in semi-arid regions can be considered as amplifiers of regional climate change by concentrating their hydrological history on one site. Lake water level changes in the Andean Altiplano during the last 20 000 years have been well documented with the support of palaeoclimatic reconstructions based on various proxies, such as diatoms, lacustrine terraces and isotopic data. For example, analysis of sedimentary cores by Cross *et al*. (2000) showed that the water surface of Lake Titicaca has fallen by about 100 m with respect to the present level between 9000 and 6500 years BP. These reconstructions are based on a proxy-lake-level transfer function. However, these reconstructions have to be confirmed by direct lake modelling, including hydrological process analysis and knowledge of atmospheric dynamics.

Investigating the influence of climatic change within the framework of the Andean Altiplano led us to quantify the different terms of the Lake Titicaca water balance and mainly to assess the role of evaporation in the overall budget. Indeed, Roche *et al*. (1992), Pouyaud (1993), Talbi *et al*. (1999) and Condom (2002) have shown that evaporation accounts for 90% of all losses, and 10% corresponds to discharge of the single outlet, the Rio Desaguadero. At a seasonal scale, direct rainfall and basin runoff contributions are mainly concentrated on the three months of the rainy season (January–March) and the maximum of Desaguadero discharge is shifted towards April (Roche *et al*., 1992). Although lake evaporation remains relatively constant, its variation presents two maxima and two minima in the year. In these conditions, annual variability of the lake level depends greatly on the monthly ratio (Rainfall + Runoff)/Evaporation, particularly during the first four months of the year when water storage is the highest. However, according to the bibliographic review by Pouyaud (1993), estimations of Lake Titicaca evaporation range widely, from 1350 mm year$^{-1}$ (Taylor and Aquize, 1984) to 1900 mm year$^{-1}$ (Richerson *et al*., 1977). In terms of water volume, this variability has to be taken into account, as this deviation corresponds approximately to a twofold discharge of the Rio

* Correspondence to: François Delclaux, IRD, UMR HydroSciences Montpellier, Université Montpelier II, Case courrier MSE 34095 Montpellier Cedex, France. E-mail: delclaux@msem.univ-montp2.fr

Desaguadero, i.e. 2·5 km$^3$ year$^{-1}$ (Roche *et al*., 1992). As a result, an accurate estimation of the evaporation rate on both the monthly and the annual scale is required for the purpose of modelling hydrological fluxes and lake level variations.

This paper has several aims. The first is to link annual variability of the lake evaporation rate to the overall meteorological data, and then to quantify the seasonal evaporation cycle at the interannual scale. To this end, we analysed the method and data as described by Carmouze (1992) in his study dedicated to the Lake Titicaca energy budget, the most documented work on the thermal dynamics of the lake. Then we compared his results on evaporation estimation with annual and seasonal data sets from other studies and observations (Landsberg, 1976; Carmouze *et al*., 1977; Richerson *et al*., 1977; Taylor and Aquize, 1984; Pouyaud, 1993; TDPS, 1993). Up to this step, special attention was paid to the radiative budget and to the heat storage/restitution. Hence, this paper broadens Carmouze's work and provides a more accurate assessment of annual evaporation flux and its seasonality.

The second aim of the paper relates to evaporation modelling. In order to analyse the water level dynamics in the past and in the future, we need an evaporation model whose input data are limited to the most relevant forcing parameters with respect to the evaporation process and which can be easily assessed in term of palaeo-reconstruction or of future climate change. Several evaporation models are reviewed and compared, with special attention given to radiative models. The optimal model in terms of the efficiency/complexity ratio is finally validated with respect to the results obtained in the first part.

## SITE DESCRIPTION AND DATA

### *Geography and climatology*

The Altiplano is a high plateau in South America. It is situated between the eastern and western Andean Cordilleras, and its altitude ranges from 3700 to 4600 m a.s.l. Its area extends over a [14 °S–66 °W] × [22 °S–71 °W] geographic window and is rather north–south oriented (Figure 1a). The climatology of this region is constrained by the yearly change in eastern and western atmospheric fluxes. It is characterized by a rainy season and a dry season (Ronchail, 1995; Berthier, 2000; Garreaud *et al*., 2003; Condom *et al*., 2004). The rainy season takes place during the austral summer, from December to March, and is characterized by an intense convective activity combined with moisture advection from the Amazon basin (Garreaud, 1999; Vuille, 1999). By way of these eastern humidity fluxes, rainfall on Lake Titicaca basin during the rainy season is about 550 mm, i.e. ∼70% of the annual amount of 800 mm. During austral winter, the eastern moist flux is replaced by westerly winds, which provide dry air related to the atmospheric stability over the Pacific Ocean. In these conditions, rainfall events are due either to the northward motion of Pacific cold fronts or to polar air intrusion along Chile (cut-offs) (Vuille and Amman, 1997; Vuille, 1999). During this 8-month dry period, the precipitation amount over the Lake Titicaca region is only about 250 mm.

### *Hydrology*

The Altiplano is a large endorheic basin (197 000 km$^2$) made up of two subcatchments: the northern Lake Titicaca basin and the southern Uyuni Salar basin (Figure 1a). Lake Titicaca, bordered by both Bolivia and

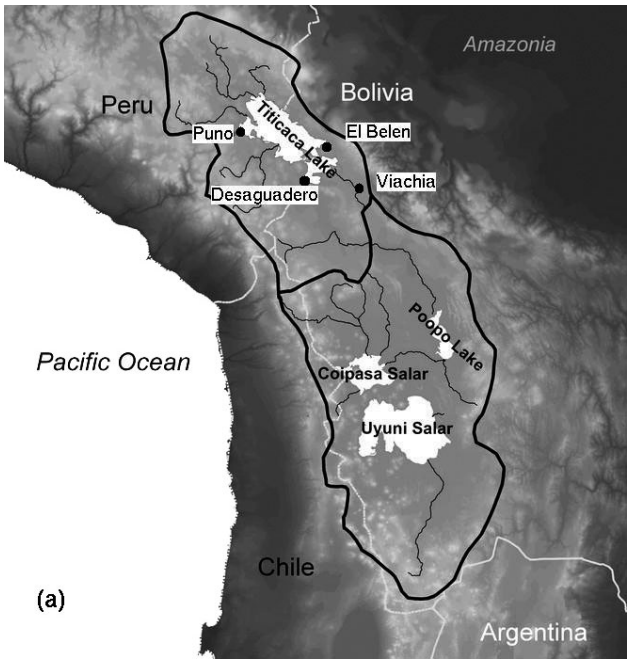


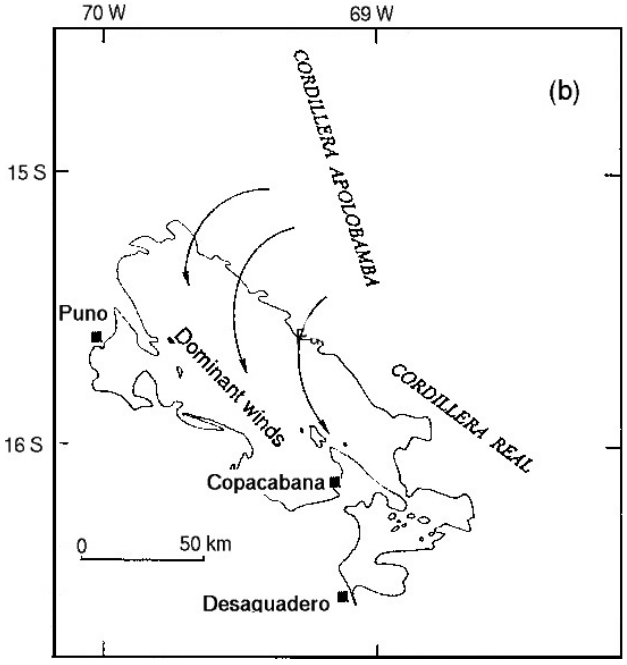


Figure 1. Location of the study area. (a) Altiplano basin and location of climatological stations; black lines are the boundaries of Titicaca (north) and Uyuni (south) basins. (b) Lake Titicaca, from Carmouze (1992): direction of dominant winds (reproduced with kind permission of Springer Science and Business Media)



DOI: 10.1002/hyp

Peru, is the largest navigable and freshwater lake in the world over 3000 m a.s.l. Through bathymetric measurements and cartographic data (Boulangé and Aquize, 1981; Wirrmann, 1992), the lake surface area is evaluated at 8560 km$^2$ at 3810 m a.s.l., and its volume is about 903 km$^3$, with a corresponding average depth of 105 m (284 m max.). The lake drains a 49 000 km$^2$ watershed whose outlet, Rio Desaguadero, supplies the southern Lake Poopo and Uyuni Salar.

Losses by infiltration and inputs from aquifers are not well documented. Infiltration has been estimated by Carmouze and Aquize (1981) as 10% of evaporation. Regarding aquifers, Roche *et al*. (1992) noted the existence of subterranean inputs, but no data are available. Thus, assuming that the underground exchange budget is low and constant, the lake mass balance is forced, on the one hand, by precipitation and basin runoff and, on the other hand, by evaporation and the Desaguadero discharge. Seasonal variation of these terms is quite high, as shown in Figure 2: inputs are highly variable in the year and loss terms are relatively constant.

Under these conditions, lake water level is very sensitive to the evaporation rate, as highlighted by a simple calculation. Given two extreme values for evaporation, i.e. 1350 mm year$^{-1}$ and 1900 mm year$^{-1}$, and all other things being equal, the lake level evolves towards two opposite states in one year, i.e. a rise and a fall by 0·37 m and 0·19 m respectively with respect to the initial value (Figure 3). This gap increases if simulation is repeated year after year.

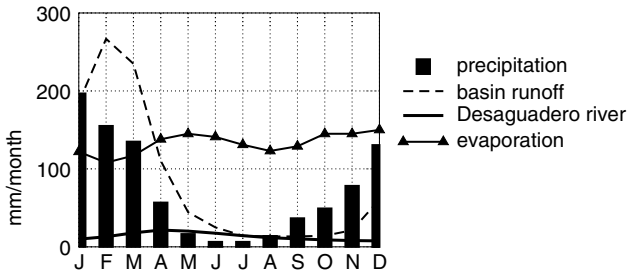


Figure 2. Interannual monthly water balance for Lake Titicaca over the period 1956–1989. Data are expressed in mm month$^{-1}$ for an average lake area of 8000 km$^2$; they come from PELT model for the evaporation (Pouyaud, 1993) and from Roche *et al*. (1992) for the other water fluxes

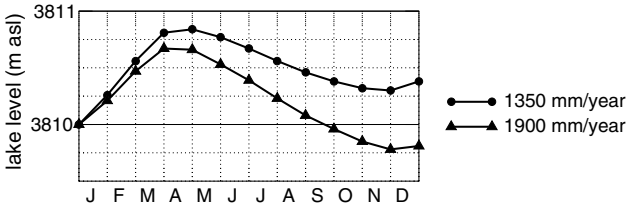


Figure 3. Monthly average simulation of Lake Titicaca level (in metres above sea level for the 1968–1987 period). Evaporation is assumed to be constant over the year with annual values of 1350 mm and 1900 mm. The monthly values of run-off, rainfall and Desaguadero discharges are interannual averages over 1968–1987 (Roche *et al*., 1992)

### *Data*

Table I shows a brief description of the data used in our study. The first data set comes from the lake energy budget described by Carmouze (1992), who estimated Lake Titicaca evaporation as a term of the water thermal balance. He used various climatic and radiative data over the period 1964–1978, as plotted in Figure 4. Furthermore, this data set has been completed with measurements of vertical water temperature profiles to allow for the thermal stratification process (Richerson, 1992).

In order to review Carmouze's radiative budget, a second data set was derived from four previous studies (Richerson *et al*., 1977; Taylor and Aquize, 1984; Vacher *et al*., 1994; Garcia *et al*., 2004). The first two relate to the Lake Titicaca evaporation and the last two are dedicated to the evapotranspiration dynamics in the Altiplano.

Another data set has been extracted from the TDPS climatological database. The TDPS system was drawn up by governments of Peru and Bolivia to address development and environmental problems concerning Lake Titicaca, Rio Desaguadero, Lake Poopo and the Coipasa Salar area (Revollo, 2001). One of the TDPS project outcomes is a hydro-climatological database handling variables such as discharge, rainfall, air temperature and pan evaporation in different locations around the lake.

Finally, monthly calculated evaporation data are available for the period 1965–1983: they come from calibration of a monthly lake water balance model achieved by

Table I. Available climatic and radiative data on study area.[a] Carmouze (1992) data are summarized in Figure 4

| Origin | Location | Period | Climatic data | Radiative data |
|---|---|---|---|---|
| Carmouze (1992) | Lake Titicaca and Puno | 1964–1978 | $T_a$, $T_w$, $e_a$, $e_w$, $U_a$, $P_a$, $N$ | $R_{ns}$, $R_{nl}$, $R_n$ |
| Richerson *et al*. (1977) | Lake Titicaca and Puno | 1973 | | $R_{ns}$, $R_{nl}$, $R_n$ |
| Taylor and Aquize (1984) | Lake Titicaca | 1973–1975 | | $R_n$ |
| Vacher *et al*. (1994) | Viachia (Bolivia) | 1988–1991 | | $R_{ns}$, $R_{nl}$, $R_n$ |
| Garcia *et al*. (2004) | Belen (Bolivia) | | $e_s - e_a$, $T_a$ | $R_{ns}$, $R_{nl}$, $R_n$ |
| TDPS | Puno (Peru) | 1964–1992 | $T_a$, $e_a$, $e_s$, $E_p$, $N$ | |
| TDPS | Desaguadero (Peru) | 1961–1992 | $T_a$, $e_a$, $e_s$, $E_p$, $N$ | |
| TDPS | Copacabana (Bolivia) | 1973–1984 | $T_a$, $e_a$, $e_s$, $E_p$, $N$ | |
| PELT | Lake Titicaca | 1965–1983 | $E$ | |

[a] $T_a$ ($T_w$) air (water) temperature, $e_a$ ($e_s$) vapour (saturation) pressure, $e_w$ saturation vapour pressure at $T_w$, $E_p$ ($E$) pan (lake) evaporation, $U_a$ wind speed, $P_a$ atmospheric pressure, $N$ nebulosity. $R_{ns}$, $R_{nl}$ and $R_n$, are net shortwave, longwave and total radiation.



DOI: 10.1002/hyp

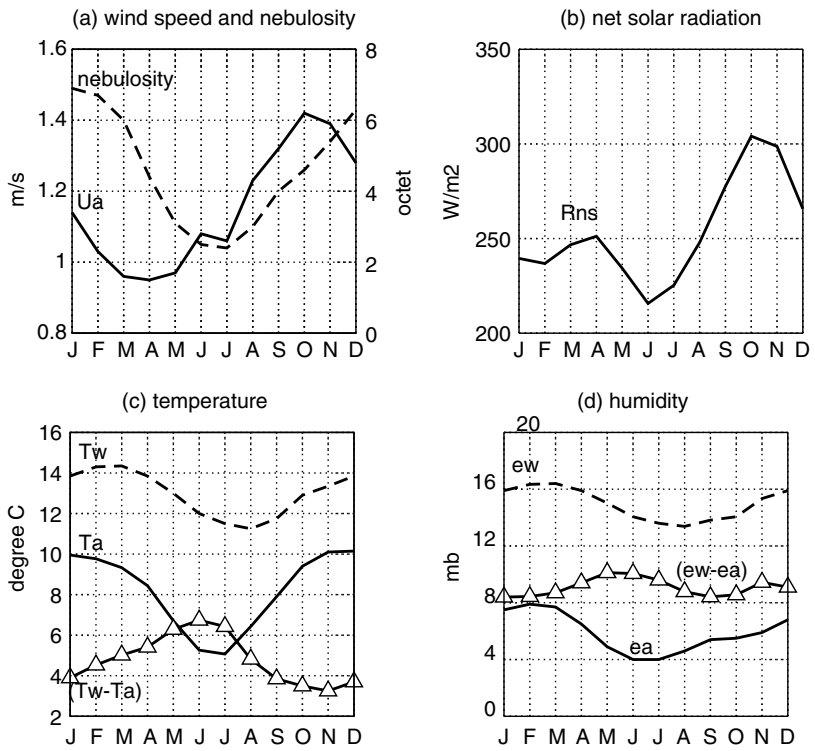


Figure 4. Monthly averages of daily climatic variables at Puno station (Peru) for the period 1964–1978 (Carmouze, 1992). (a) wind speed (m $s^{-1}$) and nebulosity (octet); (b) net shortwave radiation (W $m^{-2}$); (c) air and water surface temperatures, and their difference (°C); (d) saturation water vapour pressure, partial pressure of water vapour, and their difference (mbar). Nebulosity is expressed in octets: 1/8 for clear/cloudy sky. Wind speed is measured at 2 m above the ground and partial pressure of water vapour at 1 m above the water surface. Water temperature is the lake surface temperature

the PELT consortium (Proyecto Especial del Lago Titicaca), as reported in Pouyaud (1993).

## DISCUSSION OF THE RESULTS OF CARMOUZE

### *Methodology*

Carmouze (1992) conducted a detailed monthly thermal study of Lake Titicaca, developing the energy equation of a reference volume at the air–water interface (Pouyaud, 1986; Sene *et al*., 1991):

$$\frac{\mathrm{d}S}{\mathrm{d}t} = R_\mathrm{n} - Q - \lambda E - H + A \qquad (1)$$

where $\mathrm{d}S/\mathrm{d}t$ is the energy change, $R_\mathrm{n}$ is the net radiation flux, $Q$ is the heat exchange with deeper water in the lake, $\lambda$ is the latent heat of vaporization, $E$ is the evaporation rate, $H$ is the sensible heat flux, and $A$ is an overall heat exchange by advection. The unit of these terms is watts per square metre, except for $\lambda$ (J $kg^{-1}$) and $E$ (kg $s^{-1}$ $m^{-2}$). The variation of $\lambda$ with temperature is given by $\lambda = 2{\cdot}487 \times 10^6 - 2{\cdot}132 \times 10^3 T$, where $T$ (°C) is temperature (Xu and Singh, 2000). It should be noted that 1 W $m^{-2}$ is equivalent to 1 mm $month^{-1}$ when $T \approx 10\,^\circ\mathrm{C}$.

The contribution of $A$ can be neglected, as it accounts for low heat terms relative to water inlet/outlet, rainfall and surrounding surface effects (Sene *et al*., 1991). Then, provided that the reference volume is at equilibrium at each time step, the heat balance can be written as

$$\lambda E + H = R_\mathrm{n} - Q \qquad (2)$$

The components of net radiation $R_\mathrm{n}$ are

$$R_\mathrm{n} = R_\mathrm{ns} + R_\mathrm{nl} \qquad (3)$$

where $R_\mathrm{ns}$ is the net solar radiation (short wavelength) and $R_\mathrm{nl}$ is the net longwave radiation expressed as the difference between incoming atmospheric radiation $R_\mathrm{a}$ and outgoing water radiation $R_\mathrm{w}$.

Carmouze (1992) estimated incoming solar radiation according to the method where the maximum monthly incident radiation is modified by the ratio between the mean sunshine hours and the maximum theoretical sunshine hours. The net solar radiation $R_\mathrm{ns}$ is calculated using a water albedo value of 0·07. Atmospheric radiation $R_\mathrm{a}$ is estimated with the Brunt formula (Brutsaert, 1984), where emissivity is a linear function of the square root of atmospheric vapour pressure. Assuming that water acts like a black body, $R_\mathrm{w}$ is evaluated with the Stefan–Boltzmann equation. Long wavelength radiation ($R_\mathrm{a} - R_\mathrm{w}$) is then modified by cloud cover according to the Berliand formula (Brutsaert, 1984). Finally, Carmouze estimated $Q$ by calculating month-by-month differences of heat stored in the lake through vertical integration of temperature profiles (Richerson, 1992). Once $R_\mathrm{n}$ is computed by Equation (3), introducing the ratio between sensible and



DOI: 10.1002/hyp

latent heat fluxes, called the Bowen ratio $\beta = H/\lambda E$, makes it possible to evaluate latent heat flux $\lambda E$ according to

$$\lambda E = \frac{R_n - Q}{1 + \beta} \quad (4)$$

The Bowen ratio $\beta$ is obtained with (Brutsaert, 1984; Brunel and Buron, 1992)

$$\beta = \gamma \frac{T_w - T_a}{e_w - e_a} \quad (5)$$

where $T_w$ (°C) and $T_a$ (°C) are the water and air temperatures respectively, $e_a$ (Pa) and $e_w$ (Pa) are the vapour pressure in the air and the saturated vapour pressure at the water surface respectively, and $\gamma$ is the psychometric constant given by (Brutsaert, 1984)

$$\gamma = \frac{C_p P_a}{0{\cdot}622\lambda} \quad (6)$$

$P_a$ (Pa) is the atmospheric pressure and $C_p$ is the specific heat capacity of air ($\sim 1{\cdot}012 \times 10^3$ J kg$^{-1}$ °C$^{-1}$). $P_a$ is a function of altitude according to the formula $P_a = 1{\cdot}013 \times 10^5 - 05{\cdot}5\ z$ ($z$ in metres). Finally, as $R_n$, $Q$ and $\beta$ are known, the evaporation flux $\lambda E$ is calculated with Equation (4).

### *Analysis of energy balance*

Some results of radiative budgets from different workers are presented in Figure 5 and Table II. Owing to the high altitude of the Altiplano, shortwave radiation received by Lake Titicaca is higher that that of low-altitude lakes at the same latitude. However, during summertime, the incoming shortwave radiation is partly weakened by cloud cover, as the rainy season coincides with summer. As regards net shortwave radiation $R_{ns}$ from Carmouze, Figure 5a shows a maximum in October–November and a trough in June. Moreover, $R_{ns}$ obtained by Carmouze is close to Richerson's value (Table II). Concerning the estimation of net solar radiation by Vacher *et al.* (1994) and Garcia *et al.* (2004), it appears that lower values as listed in Table II (−27% and −23% respectively) are mainly due to a soil albedo (∼0·25) higher than that of the lake (∼0·07). In addition, seasonal variability described by correlation coefficients is consistent with that of Carmouze (Vacher *et al.* (1994): $r = 0{\cdot}80$, $n = 12$, $p < 0{\cdot}01$; Garcia *et al.* (2004):

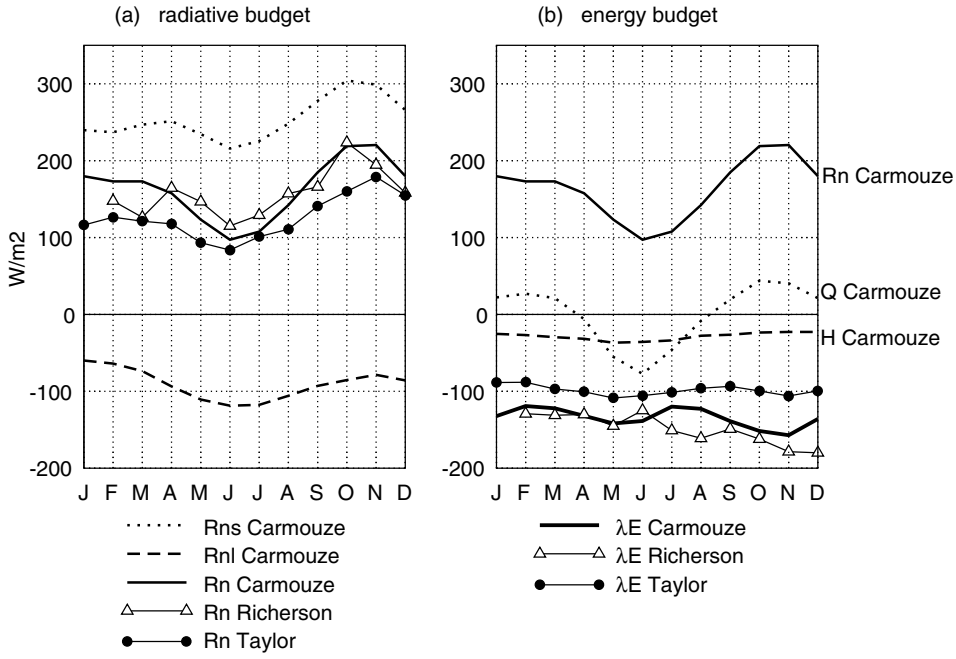


Figure 5. Monthly radiative and energy budget from Carmouze (1992), Richerson *et al.* (1977) and Taylor and Aquize (1984). (a) $R_n = R_{ns} + R_{nl}$; (b) $R_n = Q + H + \lambda E$. Units: W m$^{-2}$. Output fluxes are negative. Variables have the same meanings as mentioned in the text

Table II. Annual means of net radiative budgets according to different studies.[a] Output fluxes are negative. Richerson *et al.*'s statistics are calculated from February to December due to missing January values

| Reference | $R_{ns}$ (W m$^{-2}$) | $R_{nl}$ (W m$^{-2}$) | $R_n$ (W m$^{-2}$) | $Q$ (W m$^{-2}$) | $H$ (W m$^{-2}$) | $\lambda E$ (W m$^{-2}$) |
|---|---|---|---|---|---|---|
| Carmouze (1992) | 253·7 | −90·5 | 163·1 | 0·2 | −28·6 | −134·3 |
| Richerson *et al.* (1977) | 246·5 | −89·4 | 157·1 | −18·6 | −31·2 | −149·3 |
| Taylor and Aquize (1984) | | | 125·4 | −1·9 | −23·5 | −98·8 |
| Vacher *et al.* (1994) | 184·5 | −97·0 | 100·4 | | | |
| Garcia *et al.* (2004) | 194·3 | −66·7 | 127·5 | | | |

[a] Shortwave radiation $R_{ns}$; longwave radiation $R_{nl}$; total radiation $R_n$; lake heat storage $Q$; sensible heat flux $H$; evaporation flux $\lambda E$.



DOI: 10.1002/hyp

$r = 0{\cdot}77$, $n = 12$, $p < 0{\cdot}01$; for all the following correlations, $n = 12$ unless another value specified).

The net long wavelength radiative budget $R_{nl}$ is rather high and consistently negative as a result of low values of vapour pressure (~6 mbar), especially during winter, and as a result of the reduced thickness of the atmosphere (Garcia *et al.*, 2004). The $R_{nl}$ mean values from Carmouze (1992) and Richerson *et al.* (1977) are close together, whereas Garcia et *al.* (2004) found lower losses (+24 W m$^{-2}$); as a matter of fact, with the soil temperature being lower than the lake temperature by about 6 °C, the outgoing terrestrial radiation is weakened by ~30 W m$^{-2}$. By contrast, the $R_{nl}$ values of Vacher overestimate longwave losses with no likely explanation regarding available data.

Finally, the net radiation flux $R_n$ closely follows the pattern of the net solar radiation; it shows a maximum in October–November and a minimum in June, as illustrated in Figure 5a. Similar patterns can be observed in the Richerson *et al.* (1977) and the Taylor and Aquize (1984) results. This relationship is confirmed by the correlation coefficients between $R_n$ and $R_{ns}$ for Carmouze (1992: $r = 0{\cdot}88$, $p < 0{\cdot}001$) and for Richerson *et al.* (1977: $r = 0{\cdot}83$, $n = 11$, $p < 0{\cdot}002$). The Taylor and Aquize (1984) net radiative budget appears to be lower, but this value can be explained by a low level of solar radiation induced by a wet period, especially in 1975, as shown by the rainfall index plotted in Figure 6.

Values of sensible heat transfer $H$ from Carmouze (1992), Taylor and Aquize (1984) and Richerson *et al.* (1977) are close together, as listed in Table II. $H$, plotted in Figure 5b, is quite constant, since the air–water gradient remains stable in the year (Richerson *et al.*, 1977; Taylor and Aquize, 1984). In addition, its contribution in cooling the lake is weak, at less than 20%. Regarding the storage term $Q$, a strong seasonal variability can be seen in Figure 5b. The lake accumulates heat during the summer, with a peak at the beginning of the rainy season; afterwards, it passes through a minimum in June–July, where heat release towards the atmosphere is the highest. The $Q$ pattern is highly correlated with $R_n$, as previously described by Taylor and Aquize (1984) and as confirmed by a correlation analysis (Carmouze: $r = 0{\cdot}96$, $p < 0{\cdot}0001$; Taylor and Aquize: $r = 0{\cdot}84$, $p < 0{\cdot}001$; Richerson *et al.*: $r = 0{\cdot}9$, $n = 11$, $p < 0{\cdot}001$). Moreover, $Q$ values from Carmouze (1992) and Taylor and Aquize (1984) are close to zero, suggesting that Lake Titicaca is in thermal equilibrium at an interannual scale. By contrast, the Richerson *et al.* (1977) heat storage is strongly negative (Table II); this can be explained by the missing January value, a month that is a potential period for heating lake water.

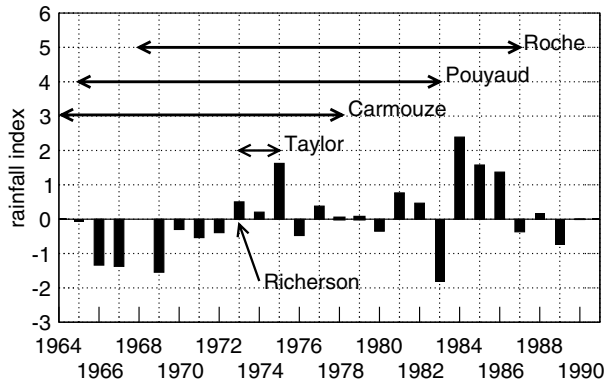


Figure 6. Rainfall index over the northern Altiplano for the 1964–1991 period. Index is calculated according to TDPS precipitation time-series

Finally, evaporation flux $\lambda E$, as plotted in Figure 5b, is the predominant factor for cooling the lake (134 W m$^{-2}$ month$^{-1}$ or 1720 mm year$^{-1}$ from Carmouze (1992)). Although it remains quite constant, it reaches two maxima in the year. The first takes place at the beginning of the rainy season (October–November), when wind speed and the humidity deficit are maximal (*cf.* Figure 4a and d). The second maximum, in May–June, is weaker; this also corresponds to a temporary maximum of humidity deficit and to the end of the heat restitution period. The two evaporation minima occur in February–March, in the heart of the rainy season, and in July–August. This double maximum pattern is quite clear for Carmouze (1992), but this trend is less obvious in the case of Taylor and Aquize (1984), for which the influence of higher rainfall remains prevailing (Figure 5b). Finally, the Richerson *et al.* (1977), evaporation flux which is about −149 W m$^{-2}$ (~1900 mm year$^{-1}$), appears to be overestimated; this value was estimated by Jacob's formula (Richerson *et al.*, 1977), whereas the water budget method applied by Richerson *et al.* (1977) in the same condition gave 1334 mm year$^{-1}$.

### *Analysis of interannual evaporation variability*

Annual Lake Titicaca evaporation as estimated by Carmouze (1992), 1720 mm year$^{-1}$, is one of the highest values we can find in the literature (Pouyaud, 1993). We examine below the possible cause of this high value by comparing it with other estimations. To this end, the available data and their sources are presented in Table III.

Comparing these values is quite tricky, since estimation periods, climatic conditions and methods do not tally. For example, the water budget method takes into account the entire lake, whereas the energy budget approach is restricted to the northern part of the lake where heat storage/restitution plays an important role because of the water depth. Moreover, Roche *et al.* (1992) emphasize how difficult it is to assess accurate terms of the water budget. In addition, the spatial variability of rainfall over the lake region is quite high and care must be taken when computing lake precipitation (Boulangé and Aquize, 1981). As calculated by Schweblin (2004), the ratio of the monthly lake rainfall to the monthly basin rainfall ranges from 1·05 to 2·08 in the year. Finally, Pouyaud (1993) argues about the relevance of the energy approach that does not take into account the geothermal flux. This process could explain the high value and the permanence of the lake bottom temperature (~11 °C), but it does not question the calculation of heat storage variation; this estimate, indeed, implicitly includes geothermal



DOI: 10.1002/hyp

Table III. Annual evaporation rates on Lake Titicaca for different periods according to different studies and methods

| Reference | Evaporation rate (mm year$^{-1}$) | Observation period | Estimation method |
|---|---|---|---|
| Taylor and Aquize (1984) | 1350 | 1973–1975 | Bulk transfer |
| Landsberg (1976) | 1480 | 1957–1961 | Water budget |
| Carmouze *et al*. (1977) | 1550 | 1956–1973 | Water budget |
| Richerson *et al*. (1977) | 1900 | 1973 | Energy budget |
| Richerson *et al*. (1977) | 1334 | 1973 | Water budget |
| Pouyaud (1993) | 1594 | 1965–1983 | Water budget |
| Roche *et al*. (1992) | 1628 | 1968–1987 | Water budget |
| Carmouze (1992) | 1720 | 1964–1978 | Energy budget |

flux because it integrates the temperature profiles (Richerson *et al*., 1977; Taylor and Aquize, 1984; Carmouze, 1992).

Nevertheless, as suggested by Roche *et al*. (1992), a connection can be found between precipitation over the lake surface and evaporation. In Figure 7, evaporation values plotted versus the lake rainfall show a clear trend. The evaporation decreases when lake rainfall increases. This feature is most probably related to the fact that humidity and nebulosity are higher during periods with large amount of rainfall: all the correlation coefficients between rainfall and humidity and between rainfall and nebulosity at the Puno, Desaguadero and Copacabana stations range between 0·91 and 0·97. Then, decreases in the humidity deficit and in the available energy at the lake surface lead to a lower evaporation flux. Concerning the evaporation rate estimation from the Richerson *et al*. (1977) heat budget, we can see in Figure 7 (dot h) that this value, 1900 mm year$^{-1}$, falls out of the trend. But it is quite difficult to consider this result as reliable, since the period concerned is only 11 months and the budget residuals are about −566 mm year$^{-1}$.

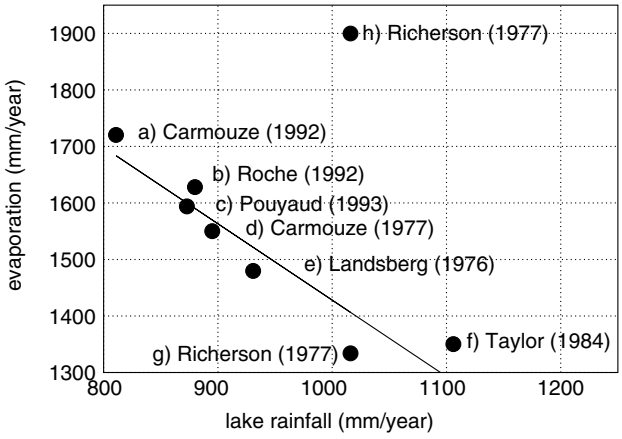


Figure 7. Evaporation versus Lake Titicaca rainfall. Interannual rainfall values are, from (a) to (g): 811, 880, 873, 895, 931, 1106 and 1016 mm year$^{-1}$. Carmouze (1992) and Taylor and Aquize (1984) rainfall values have been calculated with rain data from Boulangé and Aquize (1981). Solid line is for linear regression without taking into account the highest value from Richerson *et al*. (1977) (h)

## PAN–LAKE EVAPORATION RELATIONSHIP

In this part we investigate monthly variations of Lake Titicaca evaporation by comparing results from Carmouze (1992) with pan experimental data over the same period, 1964–1978. Observations on Class A pans located in Puno and Desaguadero meteorological stations (*cf*. map in Figure 1a and Table I) have been extracted from the TDPS database. For the analysis presented below, Copacabana station is not taken into account, as too many data are lacking.

Comparing observed and estimated evaporation fluxes as plotted in Figure 8 shows that (i) pan evaporation is greater than lake evaporation by more than 100 mm year$^{-1}$ and (ii) the range of monthly values is larger for the pans (87 and 66 mm month$^{-1}$), with only one outstanding peak, than for the lake (44 mm month$^{-1}$). This contrast, therefore, needs to be clarified in order to provide accurate lake evaporation.

The causes of the differences between pan evaporation and lake evaporation have been widely investigated (Webb, 1966; Hounam, 1973; Pouyaud, 1986; Brunel and Buron, 1992): pan lateral heat conduction, local turbulence around the pan, modification of atmospheric temperature and humidity by lake water and heat storage for deep lakes are parameters resulting in differences between pan and lake values. Several methods have been proposed to relate pan and lake evaporation. The simplest is based on the estimation of an annual proportional coefficient (Hounam, 1973; Brutsaert, 1984; Brunel and

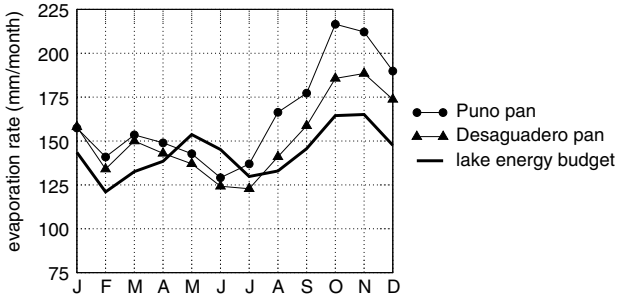


Figure 8. Seasonal evaporation derived from: (1) observations at Puno pan (1972 mm year$^{-1}$, max – min = 87 mm month$^{-1}$); (2) observations at Desaguadero pan (1817 mm year$^{-1}$, max – min = 66 mm month$^{-1}$); (3) lake energy budget (Carmouze, 1992) (1720 mm year$^{-1}$, max – min = 44 mm month$^{-1}$)



DOI: 10.1002/hyp

Buron, 1992), which depends on pan type, climatic conditions and geographic context. For example, the Class A pan coefficient varies from 0·65 in arid environments to 0·95 in equatorial climates (Brunel and Buron, 1992). Introducing a monthly variation of this coefficient sometimes improves the method (Hounam, 1973; Pouyaud, 1993), but it needs a reliable knowledge of the lake water budget. Another approach is the pan conversion method in which a pan–lake bulk transfer ratio is calculated (Brutsaert, 1984; Brunel and Buron, 1992). Webb (1966) applied this method to Lake Hefner on a daily scale. However, it requires daily monitoring of the saturation water vapour pressure. With regard to reference evapotranspiration, additional methods have been developed in order to model pan coefficients with regression equations involving climatic data (Allen *et al*., 1998). The last method is numerical simulation. Oroud (1998) simulated the heating of a sunken pan with a two-dimensional thermal model in order to assess the overestimation of pan evaporation with respect to lake evaporation in a hot and arid environment

We chose the numerical approach for linking pan and lake evaporation. Indeed, daily climatic data are quite insufficient for building a pan–lake transfer coefficient in the case of Lake Titicaca. Moreover, our objective was to estimate the evaporation rate without modelling the water budget. Thus, we developed a temperature model in which pan and lake are assumed to be free surface water volumes, with constant surface area and adiabatic edges. Because of missing data, to account for thermal stratification of the lake, we developed a simple one-dimensional energy balance model in which water temperature is assumed to be homogeneous. According to the hypotheses above, the energy equation (T model) is written as

$$h\rho C_{pw}\frac{\mathrm{d}\theta_w}{\mathrm{d}t} = \sum \Phi(\theta_w) \tag{7}$$

where $\theta_w$ (°C) is the depth average water temperature, $h$ (m) is the height of the water column, $\rho$ is the water density ($10^3$ kg m$^{-3}$), $C_{pw}$ is the specific heat capacity of water ($4{\cdot}18 \times 10^3$ J kg$^{-1}$ °C$^{-1}$) and $\sum \Phi(\theta_w)$ is the sum of energetic fluxes ($R_n - (1+\beta)\lambda E$) in watts per square metre at the air–water interface, as previously described. $R_n$ comes from Equation (3), in which $R_{ns}$ and $R_a$ are Carmouze (1992) estimations and $R_w$ is a function of $\theta_w$. $\beta$ is derived from Equation (5), and the evaporation rate $E$ is modelled by a Dalton mass transfer function (Singh and Xu, 1977):

$$E\ (\text{mm day}^{-1}) = f(U_a)(e_w - e_a) \tag{8}$$

where $U_a$ (m s$^{-1}$) is the wind speed 2 m above the surface. The empirical wind function $f$ is expressed as

$$f(U_a) = a + bU_a \tag{9}$$

where $a$ and $b$ have been locally calibrated by Carmouze (1992): $a = 0{\cdot}17$ and $b = 0{\cdot}30$.

Simulations were carried out according to two $h$ values: (1) $h = 0{\cdot}20$ m for a Class A pan; (2) $h =$ 40 m for the lake, as this depth is the mean water layer depth governed by seasonal temperature variation (Richerson, 1992). For pan simulations, the model is forced by pan station climatic data when available. Equation (7) is then integrated at a daily time step with a fifth-order Runge–Kutta method for a climatological year corresponding to 1964–1978. The results are reported in Figure 9.

Pan evaporation is plotted in Figure 9a and b. Simulated evaporations correctly account for seasonal variability (one peak in the year). Moreover, simulated evaporations are in agreement with local conditions that are different for the two stations. Reviewing the climatic data shows that Desaguadero station is colder (by $-2$ °C in July) and wetter (by 1 mbar over the year) than Puno station, contributing to a lower Desaguadero evaporation rate ($-155$ mm year$^{-1}$), as plotted in Figure 8. However the simulated evaporations of Puno and Desaguadero are underestimated by 11% and 5% respectively. This difference is undoubtedly related to local phenomena that are not documented and not taken into account in the model. Among them, the strength and the variability of wind are certainly key parameters. Nevertheless, simulations confirm the prevailing role of solar radiation on pan evaporation: correlation coefficients between solar radiation (Figure 4b) and measured evaporation in Puno and Desaguadero stations are $r = 0{\cdot}96$ ($p < 0{\cdot}0001$) and $r = 0{\cdot}92$ ($p < 0{\cdot}0001$) respectively.

Comparison of the simulations of pan and lake cases by the T model ($h = 0{\cdot}20$ m and $h = 40$ m) emphasizes the importance of thermal inertia, as shown in Figure 9a–c. Summer heat storage and winter release narrows the evaporation range, leading to a decrease in the maximum–minimum interval of monthly values from about 90 mm month$^{-1}$ for the pans to about 30 mm month$^{-1}$ for the lake. Moreover, lake evaporation seasonality is less correlated with solar radiation than with the pan. Heat storage/restitution reduces fluctuation of the water surface temperature and thereby variability of saturation deficit. More accurately, the evolution of the lake surface temperature during the heat restitution period leads to an increase in humidity deficit and, consequently, to a second evaporation maximum in May–June. Figure 9c shows a good agreement between evaporation simulated by the T model and evaporation originally from the energy budget, both in terms of seasonality ($r = 0{\cdot}75$, $p < 0{\cdot}01$) and total evaporation (0·8%). Simulation output additionally complies with the evaporation estimate as calibrated by the PELT team and based on the lake water balance (Pouyaud, 1993): the double seasonal peak is confirmed, even if the PELT value (Pouyaud, 1993) is lower (1594 mm year$^{-1}$), due to a more rainy period, as previously outlined (Figure 7).

As shown in Figure 9d, lake temperature variability is correctly simulated by the T model ($r = 0{\cdot}89$, $p < 0{\cdot}001$; deviation $\delta = 0{\cdot}28$ °C). Nevertheless, for the period from March to June, the simulated lake temperature is delayed



DOI: 10.1002/hyp

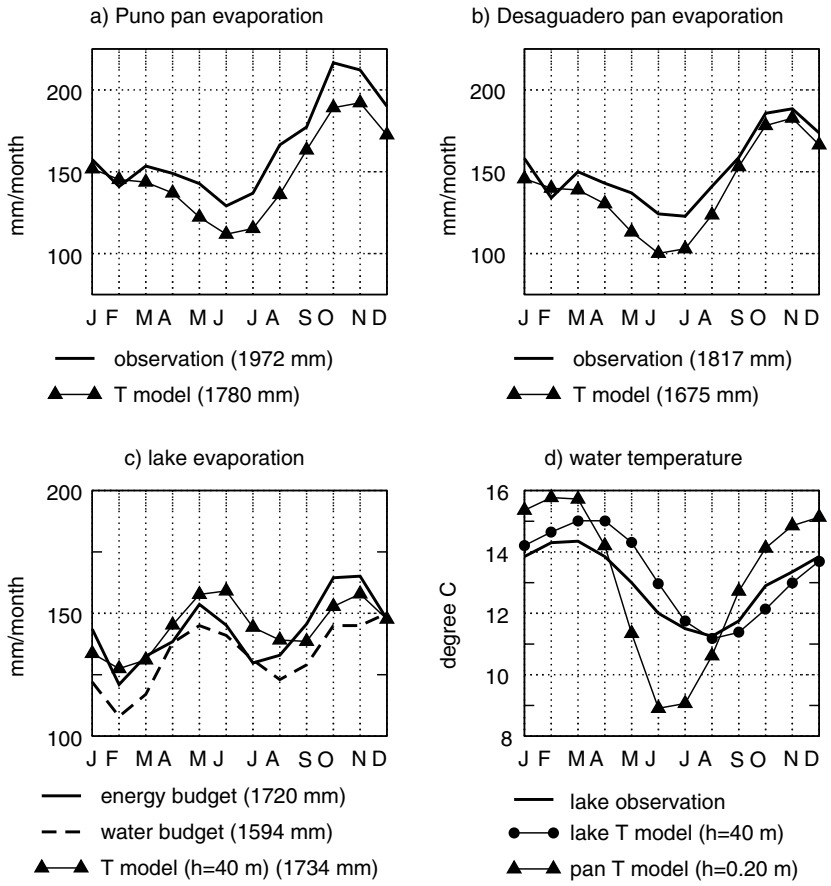


Figure 9. Simulation of monthly evaporation and temperature of a water volume with a thermal model (T model) under 1964–1978 climatic conditions. $h$ is the depth of the water volume. (a) and (b) observed and simulated ($h = 0{\cdot}20$ m) evaporation of Puno and Desaguadero pans; (c) lake evaporation from energy budget (Carmouze, 1992), from PELT water budget (Pouyaud, 1993), and from T model (d) observed and simulated lake and pan temperatures. Values between parentheses are annual values in millimetres

by a month with respect to the observed one. This can be explained by the different thermal inertia between the model configuration and the actual lake body. In the model, the depth of the homogeneous temperature water layer is prescribed to a constant 40 m value. In the lake, this value varies in time according to the annual cycle of stratification (Richerson, 1992). During the heat restitution period, which is the same as the de-stratification period, thermal inertia simulated by the model is higher than for the lake. Additional computations with $h = 20$ m and $h = 30$ m show that the 1 month delay disappears. With regard to pan temperature (Figure 9d), experimental data are unavailable, but the high pan thermal dynamics as simulated are consistent with the lower variability of lake temperature.

Lastly, a sensitivity analysis was carried out by introducing geothermal flux. According to Pouyaud (1993), the high temperature of the lake bottom (11 °C instead of 4 °C) is induced by terrestrial heat flow. Its value was estimated at $60 \times 10^{-3}$ W m$^{-2}$ by Sclater *et al.* (1970) as part of a measurement survey of sediment temperature. However, introducing this heat contribution in the T model does not modify the upper layer thermal budget on the time-scales we are concerned with.

At this point in our work, we consider the Carmouze (1992) evaporation results as fully validated. Although accuracy of experimental data is lacking, Carmouze results are compatible with data coming from various sources. Carmouze radiative budget is consistent with other ones. It clearly underlines the role of lake heat storage/restitution on the evaporation at a seasonal scale. Moreover, Carmouze annual evaporation, which appears to be one of the highest in the literature, can be explained by the dryness of the study period. Finally, although the patterns of pan and lake monthly evaporation seem to be unrelated, a simple temperature model shows that the Carmouze (1992) estimation is consistent with pan observations, even if some significant variable such as wind is not sufficiently documented. Consequently, the monthly evaporation rate coming from the Carmouze (1992) energy budget is reliable enough to be used in the modelling step.

## MODELLING EVAPORATION

### *Model review*

In order to validate an evaporation model of past or future climate, we discarded models with explicit water characteristics such as water temperature. By contrast, models were reviewed with an eye towards methods founded on radiative and atmospheric forcing variables;



DOI: 10.1002/hyp

these variables are indeed among the best documented for the past and can be obtained from various studies in domains such as climate modelling (Braconnot *et al*., 2000; Garreaud *et al*., 2003), isotopic data (Coudrain *et al*., 2002) and palaeohydrology (Hastenrath and Kutzbach, 1985).

According to the study conducted by Xu and Singh (2000), who focused on a set of generalized radiation-based evaporation equations, five models were selected: the Makkink, Doorenbos–Pruitt, Hargreaves, Jensen–Haise, and Abtew models. The corresponding forcing variables are limited to solar radiation and air temperature, except for the Doorenbos–Pruitt equation, which also requires wind speed and relative humidity. In order to compare these equations with more classical formulae, three other models were considered: Penman (Sene *et al*., 1991; Vallet-Coulomb *et al*., 2001), Priestley–Taylor (Priestley and Taylor, 1972; Xu and Singh, 2000) and Dalton as calibrated by Carmouze (1992). These models and related parameters are all presented in Table IV.

In order to improve the net radiation $R_n$ parameterization, the longwave radiation budget was determined according to Sicart (2002), who carefully calibrated the energy balance of Zongo Glacier (less than 150 km east of Lake Titicaca): atmospheric radiation $R_a$ was modelled with the Brutsaert formula (Brutsaert, 1975), where emissivity is proportional to $(e_a/T_a)^{1/7}$. The cloud effect was parameterized as $(1 + \alpha n^{\beta})$, where $n$ is the cloud cover derived from the ratio (solar radiation)/(extraterrestrial radiation). $\alpha$ and $\beta$ are calibrated values equal to 0·4 and 1·0 respectively.

Figure 10 summarizes the results from the different models and Table V gathers statistics of the comparison between models and energy budget evaporation. The Carmouze (1992) model, which was calibrated with estimated values, gives good results on annual and monthly scales (Figure 10a). The Penman and Priestley–Taylor equations are in full agreement with estimated values as well (Figure 10b and c, Table V (models b, c and c′)) in terms of correlation and deviation, but a bias was introduced in these calculations: on the one hand, estimated evaporation comes from the energy budget including a net radiation calculation; on the other hand, the same net radiation is involved in the equations. Thus, obtaining good agreement between estimated and modelled evaporation values is very consistent and not entirely unexpected. However, the Penman approach gives further information, as it divides overall evaporation into radiative and aerodynamic components. For Lake Titicaca, the radiation contribution prevails (83%), which is consistent with the 74% ratio from Garcia *et al*. (2004) for Belen station (Bolivia). As highlighted by Garcia *et al*. (2004), such a difference is due to a dryness effect: the radiation contribution is lower in a location such as Belen (where rainfall is about 466 mm year$^{-1}$) than in a wetter place, e.g. Puno or Desaguadero (where rainfall is about 675 mm year$^{-1}$).

Owing to the lake altitude, a sensitivity analysis on the influence of elevation on the Penman aerodynamic term was carried out according to the following multiplicative function: $f(z) = 1 + 10^{-5}\, z$ ($z$ in metres; Sene *et al*., 1991). However, its impact is quite low, as it increases the modelled evaporation by +1·8% with respect to estimated values.

The behaviour of radiative models is quite variable. Hargreaves and Jensen–Haise functions (Figure 10e and g), where air temperature is explicitly taken into account, strongly underestimate evaporation, as shown

Table IV. Eight evaporation equations and their coefficient values[a]

| Model | Evaporation rate equation | Coefficient values[b] | |
|---|---|---|---|
| (a) Carmouze | $(a + bU_a)(e_w - e_a)$ | $a = 1{\cdot}97 \times 10^{-11}$ m s$^{-1}$ Pa$^{-1}$ | ($a = 0{\cdot}17$) |
| | | $b = 3{\cdot}47 \times 10^{-11}$ Pa$^{-1}$ | ($b = 0{\cdot}30$) |
| (b) Penman | $\frac{\Delta}{\Delta+\gamma}\frac{R_n - Q}{\rho\lambda} + \frac{\gamma}{\Delta+\gamma} f(U_a)(e_s - e_a)$ | $f(U_a) = c(a + bU_a)$ | |
| | | $a = 1{\cdot}16 \times 10^{-10}$ m s$^{-1}$ Pa$^{-1}$ | ($a = 1$) |
| | | $b = 6{\cdot}25 \times 10^{-11}$ Pa$^{-1}$ | ($b = 0{\cdot}54$) |
| | | $c = 0{\cdot}26$ | |
| (c) Priestley–Taylor | $a\frac{\Delta}{\Delta+\gamma}\frac{R_n - Q}{\rho\lambda} + b$ | $a = 1{\cdot}26$, $b = 0$ m s$^{-1}$ | ($b = 0$) |
| (d) Makkink | $a\frac{\Delta}{\Delta+\gamma}\frac{R_{ns}}{\rho\lambda} + b$ | $\mathbf{a = 0{\cdot}98, b = 1{\cdot}09 \times 10^{-8}}$ **m s$^{-1}$** | **($b = 0{\cdot}94$)** |
| | | $a = 0{\cdot}61$, $b = -1{\cdot}39 \times 10^{-10}$ m s$^{-1}$ | ($b = -0{\cdot}012$) |
| (h) Doorenbos–Pruitt | | $\mathbf{a = 0{\cdot}77, b = 2{\cdot}31 \times 10^{-9}}$ **m s$^{-1}$** | **($b = 0{\cdot}2$)** |
| | | $a = a(H_r, U_a)$ | |
| (e) Hargreaves | $a(T_a + b)\frac{R_{ns}}{\rho\lambda}$ | $b = -3{\cdot}47 \times 10^{-9}$ m s$^{-1}$ | ($b = -0{\cdot}3$) |
| | | $a = 0{\cdot}0135\,^{\circ}\mathrm{C}^{-1}$, $b = 17{\cdot}8\,^{\circ}\mathrm{C}$ | |
| | | $\mathbf{a = 0{\cdot}0145\,^{\circ}C^{-1}, b = 17{\cdot}8\,^{\circ}C}$ | |
| (g) Jensen–Haise | | $a = 0{\cdot}025\,^{\circ}\mathrm{C}^{-1}$, $b = 3\,^{\circ}\mathrm{C}$ | |
| (f) Abtew | $a\frac{R_{ns}}{\rho\lambda}$ | $a = 0{\cdot}53$ | |

[a] $\Delta$ is an approximation of $de_w/dT$ at the air temperature and $\gamma$ is the psychrometric constant. $\rho$ is the density of water (1000 kg m$^{-3}$). Units: evaporation rate and $U_a$ (wind speed at 2 m above the surface) are in m s$^{-1}$; $e_w$, $e_s$ and $e_a$ are in Pa; $H_r$ (relative humidity) is in %; $T_a$ is in °C; $\lambda$ is in J kg$^{-1}$; $\Delta$ and $\gamma$ are in Pa °C$^{-1}$; $R_n$, $Q$ and $R_{ns}$ are in W m$^{-2}$.

[b] Coefficients in bold have been recalibrated by Xu and Singh (2000). Coefficients in parentheses are values that can be found in the literature where evaporation and pressure are expressed in mm day$^{-1}$ and mbar.



DOI: 10.1002/hyp

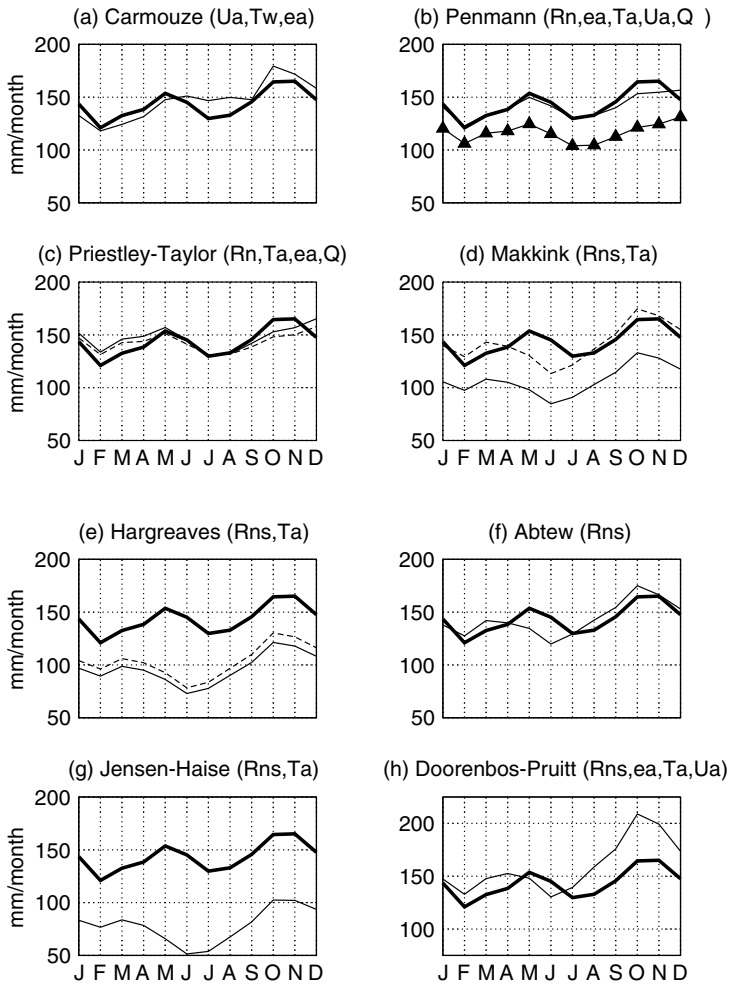


Figure 10. Results of evaporation models as described in Table IV. Variables in parentheses are input variables required by each model. Thick lines are evaporation data from energy budget by Carmouze (1992); thin lines are model results; dashed lines are recalibrated models results (Xu and Singh, 2000); up-triangle curve in Penmann graph (b) is the simulated radiative contribution to overall evaporation

Table V. Simulation results of Lake Titicaca evaporation rates according to the models described in Table IV. Results from radiative models are listed in the second part of the table. Statistics $r$, $p$-value and deviation $\delta$ have been calculated with respect to evaporation rate estimated from energy budget. It can be noted that model efficiency is improved in the case of recalibrated models

| Model | $r$ | $p$-value | $\delta$ (%) |
|---|---|---|---|
| (a) Carmouze | 0·83 | 0·0008 | 2·3 |
| (b) Penman | 0·92 | 0·000 02 | −1·4 |
| (c) Priestley–Taylor | 0·74 | 0·006 | 2·4 |
| (c′) Priestley–Taylor, recalibrated by Xu and Singh (2000) | 0·74 | 0·006 | −0·3 |
| (d) Makkink | 0·67 | 0·018 | −25·2 |
| (d′) Makkink, recalibrated by Xu and Singh (2000) | 0·67 | 0·017 | −1·0 |
| (h) Doorenbos–Pruit | 0·77 | 0·003 | 11·3 |
| (e) Hargreaves | 0·63 | 0·027 | −32·7 |
| (e′) Hargreaves, recalibrated by Xu and Singh (2000) | 0·63 | 0·027 | −27·7 |
| (g) Jensen–Haise | 0·55 | 0·065 | −45·3 |
| (f) Abtew | 0·71 | 0·01 | 0·1 |

by deviation values (Table V, models e, e′ and g). These results are confirmed by Xu and Singh (2000), whose investigations showed an underestimation of winter evaporation for these models in Switzerland, where the air temperature is similar to Lake Titicaca air temperature. Similarly, an intercomparison study carried out by Vacher *et al*. (1994) on modelling potential evapotranspiration in the Bolivian Altiplano indicated that the results from the Hargreaves approach were among the lowest potential evapotranspiration estimations. Underestimation has also been found by Garcia *et al*. (2004).

The Doorenbos–Pruitt function (Figure 10h) can be



DOI: 10.1002/hyp

considered as a substitution model of the Penman approach when wind and humidity values are not known with enough confidence (Xu and Singh, 2000). Regarding the statistics of the model outputs in Table V (model h), this approach could be considered as acceptable. However, according to the outstanding peak in Figure 10h, evaporation calculated in this way describes a Class A pan evaporation process rather than a lake evaporation process.

Finally, the two radiative models are the most consistent with the Carmouze (1992) data: the Abtew model (Figure 10f, Table V, model f), which is only forced by solar radiation, and the recalibrated Makkink model (Figure 10d, Table V, model d′), whose input variables are solar radiation and air temperature. The very low values of deviation of annual evaporation (−1% and 0·1% in Table V) show that solar radiation is the main forcing variable controlling evaporation at an annual scale. This result is consistent with the previously described trend: the lower the rainfall, the higher the solar radiation, the higher the evaporation. However, these models do not take into account the thermal storage/restitution cycle of the lake; these models, indeed, induce a forward shift in the simulated curve by 1 to 2 months between April and July, i.e. the period when the solar radiation is decreasing (*cf.* Figure 4b). In the case of the Makkink model, this effect is reinforced by the $\Delta/\Delta + \gamma$ term, which reaches a minimum (−10% with respect to its mean value) in July–August, inducing a higher deviation than for the Abtew model.

## CONCLUSIONS

As evaporation accounts for 90% of Lake Titicaca water output, it constitutes a major component of the lake water balance. Characteristics of the evaporation rate are related to the specific features of the lake. First, the geographic situation at low latitudes (16 °S) and the large water volume of the lake substantially constrain evaporation on a seasonal scale, not only in terms of radiative and climatic conditions, but also because of the lake thermal inertia (Taylor and Aquize, 1984; Carmouze, 1992). Furthermore, spatial variability of meteorological conditions plays an important role in this mountainous area. An evaporation study in such a framework, therefore, requires various and simultaneous data time-series over long periods, but these data sets are rarely available. Our results on the various questions raised by the estimation of the Lake Titicaca evaporation are summarized below.

First, annual evaporation is quite high (about 1500 mm year$^{-1}$) for a mountain lake where temperatures are quite low. This value is mainly explained by the air dryness, inducing a rather high vapour pressure deficit. This effect is emphasized by the unusually hot surface water (∼13 °C). Carmouze (1992) demonstrated that if the water was at the same temperature as the air, then evaporation would decrease by 40%.

The second point is concerned with the large range of annual evaporation estimations, between 1300 and 1900 mm year$^{-1}$. Gathering the published data, we underlined that the annual evaporation decreases when the annual lake rainfall increases (from 800 to 1100 mm year$^{-1}$). The scope of this result is limited, since available data are several-year averages. Furthermore, assessing accurate lake rainfall is quite complex, as local meteorological processes increase the lake precipitation. Nevertheless, this relationship expresses the overall trend by which increasing rainfall is related to an increasing humidity and leads to a decrease in evaporation.

The third question refers to assessing seasonal evaporation and linking pan and lake evaporations. First, we verified the reliability of the radiative and heat budget of Lake Titicaca as described by Carmouze (1992). Comparing data from various studies (Richerson *et al.*, 1977; Taylor and Aquize, 1984; Vacher *et al.*, 1994; Garcia *et al.*, 2004) shows that the Carmouze (1992) outcomes are consistent with other results in spite of mismatching study periods. Net radiation balance exhibits a peak at the beginning of the rainy season (October–November) and a trough in the heart of winter (June) (Richerson *et al.*, 1977). The sum of lake heat storage and restitution (null at the annual scale) is strongly correlated to the net radiation balance (Taylor and Aquize, 1984). As latent and sensible heat fluxes are negative throughout the year, they are the lake cooling terms. Sensible heat flux, which is quite constant over the year, is one-fifth of the evaporation flux. Second, we focused on the seasonality of evaporation, which presents two maxima in the year (Carmouze, 1992). One of these occurs at the beginning of the rainy season (October–November) when solar radiation and wind speed are at a maximum. The second, in May–June, is mainly due to a local maximum of the humidity deficit when heat stored in the lake during summer is released into the atmosphere. Accordingly, water temperature and humidity deficit are higher than they would be without this thermal restitution. This result was confirmed when addressing the comparison with pan evaporation, where only one maximum can be observed and where the evaporation rate is higher by about 100 mm year$^{-1}$ than that of the lake. In order to link pan and lake evaporation, a simple thermal model of a water volume was developed. Its aim was to simulate the scale effect when passing from a pan to a deep lake even if the hypotheses do not account for processes such as atmospheric turbulence, lateral fluxes and thermal stratification. Despite these limits, the thermal model correctly describes the pan evaporation seasonality: a high correlation with solar radiation, with a minimum in June and a maximum in October–November. Concerning the lake temperature, the thermal model results agree with the actual measurements. Nevertheless, the model is not completely efficient. The water depth with a homogeneous temperature is supposed to be constant (40 m) in the model, whereas in reality it varies, according to the stratification effect, from a few metre to 50 m over the



DOI: 10.1002/hyp

year (Richerson, 1992). Finally, the simulated lake evaporation obtained with a 40 m water depth complies with data derived by Carmouze (1992) in terms of variability and average: it confirms that thermal inertia and related storage/release processes are critical to the dynamics of lake evaporation at the monthly scale.

The last point of our study concerns evaporation modelling of Lake Titicaca. We tested models likely to be used in a palaeo-climatological context. For this reason, we focused on five simple models, based on a radiative approach (Xu and Singh, 2000) in which forcing variables are solar radiation and air temperature. It appears that the most efficient models are the Abtew model and the Makkink model, both in terms of deviation and in terms of correlation. The Abtew evaporation is simply proportional to the net solar radiation, whereas the Makkink formulation takes into account air temperature by the factor $\Delta/\Delta + \gamma$. These two models cannot simulate the heat storage/release cycle because they are strongly correlated with the net radiation, and not with the solar radiation. As a result, calculated evaporation is in advance by about 2 months in winter. Apart from this period, these two models correctly capture the annual total and seasonal variability. These two models can, therefore, be recommended for further palaeo-climatological studies.

## ACKNOWLEDGEMENTS

We wish to acknowledge financial support of the research unit HydroSciences Montpellier (HSM). Furthermore, we thank Great Ice, a research unit of IRD (Institut de Recherche pour le Developpement) and SENHAMI of Peru and Bolivia (Servicio Nacional de Hydro-Meteorologia) for their help in data gathering.

## REFERENCES

Allen G, Pereira LS, Raes D, Smith M. 1998. *Crop Evapotranspiration. Guidelines for Computing Crop Water Requirements. FAO Irrigation and Drainage Paper* No. 56. FAO: Rome, Italy.

Berthier E. 2000. *Modélisation méso-échelle du climat sud américain*. DEA Report, Laboratoire des Sciences du Climat et de l'Environnement, France.

Boulangé B, Aquize E. 1981. Morphologie, hydrographie et climatologie du lac Titicaca et de son bassin versant. *Revue d'Hydrobiologie Tropicale* **14**(4): 269–287.

Braconnot P, de Vernal A, Joussaume S, Taylor K. 2000. Paleoclimate modeling intercomparison project. In *Proceedings of the Third PMIP Workshop*, October 1999, La Huardière, Canada. Braconnot P (ed.). WMO/ICPO Publication Series No. 34.

Brunel JP, Bouron B. 1992. *Évaporation des nappes d'eau libre en Afrique sahélienne et tropicale*. Rapport, CIEH-ORSTOM, Paris, France.

Brutsaert W. 1975. On a derivable formula for long-wave radiation from clear skies. *Water Resources Research* **11**(5): 742–744.

Brutsaert W. 1984. *Evaporation into the Atmosphere*. Reidel: Dordrecht, Holland.

Carmouze JP. 1992. The energy balance. In *Lake Titicaca, a Synthesis of Limnological Knowledge*, Dejoux C, Iltis A (eds). Kluwer: 131–146.

Carmouze JP, Aquize E. 1981. La régulation hydrique du lac Titicaca et l'hydrologie de ses tributaires. *Revue d'Hydrobiologie Tropicale* **14**(4): 311–328.

Condom T. 2002. *Dynamiques d'extension lacustre et glaciaire associées aux modifications du climat dans les Andes Centrales*. PhD thesis, Université Paris VI, Paris.

Carmouze JP, Arze C, Quintanilla J. 1977. La régulation hydrique des lacs Titicaca et Poopo. *Cahiers ORSTOM, Série Hydrobiologique* **XI**(4): 269–283.

Condom T, Coudrain A, Dezetter A, Brunstein D, Delclaux F, Sicart JE. 2004. Transient modelling of lacustrine regressions: two case studies from the Andean Altiplano. *Hydrological Processes* **18**: 2395–2408.

Coudrain A, Loubet M, Condom T, Talbi A, Ribstein P, Pouyaud B, Quintanilla J, Dieulin C, Dupre B. 2002. Données isotopiques ($^{87}Sr/^{86}Sr$) et changements hydrologiques depuis 15 000 ans sur l'Altiplano andin. *Hydrological Sciences Journal* **47**(2): 293–306.

Cross SL, Baker PA, Seltzer GO, Fritz SC, Dunbar RB. 2000. A new estimate of the Holocene lowstand level of Lake Titicaca, central Andes, and implications for tropical palaeohydrology. *The Holocene* **10**(1): 21–32.

Garcia M, Raes D, Allen R, Herbas C. 2004. Dynamics of reference evapotranspiration in the Bolivian highlands (Altiplano). *Agricultural and Forest Meteorology* **125**: 67–82.

Garreaud R. 1999. Multiscale analysis of the summertime precipitation over the Central Andes. *Monthly Weather Review* **127**: 901–921.

Garreaud R, Vuille M, Clement AC. 2003. The climate of the Altiplano: observed current conditions and mechanisms of past changes. *Palaeogeography, Palaeoclimatology, Palaeoecology* **194**: 5–22.

Hastenrath S, Kutzbach J. 1985. Late Pleistocene climate and water budget of the South America Altiplano. *Quaternary Research* **24**: 249–256.

Hounam CE. 1973. *Comparison between pan and lake evaporation*. WMO Technical Note no. 126, WMO, Geneva, Switzerland.

Landsberg HE. 1976. Climates of Central and South America. In *World Survey of Climatology*, vol. 12, Schwerdtfeger W (ed.). Elsevier.

Oroud IM. 1998. The influence of heat conduction on evaporation from sunken pans in hot, dry environment. *Journal of Hydrology* **210**: 1–10.

Pouyaud B. 1986. Contribution à l'évaluation de l'évaporation de nappes d'eau libre en climat tropical sec. Thèse d'Etat. In *Collection Etudes et Thèses*. IRD Editions: Paris.

Pouyaud B. 1993. *Lago Titicaca. Programa estudios TDPS: mission d'évaluation sur la prise en compte de l'évaporation*. GIE Hydro Consult International, GIE ORSTOM-EDF.

Priestley CHB, Taylor RJ. 1972. On the assessment of the surface heat flux and evaporation using large scale parameters. *Monthly Weather Review* **100**: 81–92.

Revollo MM. 2001. Management issues in the Lake Titicaca and Lake Poopo system: importance of developing a water budget. *Lakes & Reservoirs: Research and Management* **6**: 225–229.

Richerson PJ. 1992. The thermal stratification regime in Lake Titicaca. In *Lake Titicaca, a Synthesis of Limnological Knowledge*, Dejoux C, Iltis A (eds). Kluwer: 120–130.

Richerson PJ, Widmer C, Kittel T. 1977. *The Limnology of Lake Titicaca (Peru-Bolivia), a Large, High Altitude Tropical Lake. Institute of Ecology Publication* 14. Institute of Ecology, University of California: Davis, CA.

Roche MA, Bourges J, Cortes J, Mattos R. 1992. Climatology and hydrology of the Lake Titicaca basin. In *Lake Titicaca, a Synthesis of Limnological Knowledge*, Dejoux C, Iltis A (eds). Kluwer: 63–88.

Ronchail J. 1995. L'aridité sur l'Altiplano bolivien. *Sécheresse* **6**: 45–51.

Sclater JG, Vacquier V. Rohrhirsch JH. 1970. Terrestrial heat flow measurements on Lake Titicaca, Peru. *Earth and Planetary Science Letters* **8**: 45–54.

Schweblin M. 2004. *Modélisation conceptuelle de dynamiques lacustres sur l'Altiplano Andin*. Engineer report, Ecole d'Hydraulique et de Mécanique de Grenoble.

Sene KJ, Gash JHC, McNeil DD. 1991. Evaporation from a tropical lake: comparison of theory with direct measurements. *Journal of Hydrology* **127**: 193–217.

Sicart JE. 2002. *Contribution à l'étude des flux d'énergie, du bilan de masse et du débit de fonte d'un glacier tropical: le glacier du Zongo*. PhD thesis, Université Paris VI, Paris.

Singh VP, Xu CY. 1997. Evaluation and generalization of 13 mass-transfer equations for determining free water evaporation. *Hydrological Processes* **11**: 311–323.

Talbi A, Coudrain A, Ribstein P, Pouyaud B. 1999. Calcul de la pluie sur le bassin-versant du lac Titicaca pendant l'Holocène. *Comptes Rendus de l'Accadémie des Sciences, Paris, Sciences de la Terre et des Planètes* **329**: 197–203.

Taylor M, Aquize E. 1984. A climatological energy budget of Lake Titicaca (Peru/Bolivia). *Internationale Vereinigung für Theoretische und Angewandte Limnologie, Verhandlungen* **22**: 1246–1251.

TDPS. 1993. *Gestor del banco de datos hidrometeorologicos del sistema TDPS*, La Paz.

Vacher JJ, Imana E, Canqui E. 1994. Las caracteristicas radiativas y la evapotranspiracion potencial en el Altiplano boliviano. *Revista de Agricultura, Facultad de Ciencias Agricolas y Pecuarios, UMSS Cochamba, Bolivia* **50**(24): 4–11.

Vallet-Coulomb C, Legesse D, Gasse F, Travi Y, Chernet T. 2001. Lake evaporation estimates in tropical Africa (Lake Ziway, Ethiopia). *Journal of Hydrology* **245**: 1–18.

Vuille M. 1999. Atmospheric circulation over the Bolivian Altiplano during dry and wet periods and extreme phases of the southern oscillation. *International Journal of Climatology* **19**: 1579–1600.

Vuille M, Amman C. 1997. Regional snowfall patterns in the high, arid Andes. *Climatic Change* **36**: 413–423.

Webb EK. 1966. A pan–lake evaporation relationship. *Journal of Hydrology* **4**: 1–11.

Wirrmann D. 1992. Morphology and bathymetry. In *Lake Titicaca, a Synthesis of Limnological Knowledge*, Dejoux C, Iltis A (eds). Kluwer: 16–22.

Xu CY, Singh VP. 2000. Evaluation and generalization of radiation-based methods for calculating evaporation. *Hydrological Processes* **14**: 339–349.




DOI: 10.1002/hyp